Biomaterials Science

ROYAL SOCIETY OF CHEMISTRY

PAPER

View Article Online
View Journal | View Issue

Cite this: *Biomater. Sci.*, 2024, **12**, 2943

An injectable fluorescent and iodinated hydrogel for preoperative localization and dual image-guided surgery of pulmonary nodules†

Woojin Back,‡[a] Jiyun Rho,‡[b,c] Kyungsu Kim,[b,c] Hwan Seok Yong,[d] Ok Hwa Jeon,[b,c] Byeong Hyeon Choi,[b,c] Hyun Koo Kim*[b,c] and Ji-Ho Park *[a]

The widespread use of video-assisted thoracoscopic surgery (VATS) has triggered the rapid expansion in the field of computed tomography (CT)-guided preoperative localization and near-infrared (NIR) fluorescence image-guided surgery. However, its broader application has been hindered by the absence of ideal imaging contrasts that are biocompatible, minimally invasive, highly resolvable, and perfectly localized within the diseased tissue. To achieve this goal, we synthesize a dextran-based fluorescent and iodinated hydrogel, which can be injected into the tissue and imaged with both CT and NIR fluorescence modalities. By finely tuning the physical parameters such as gelation time and composition of iodinated oil (X-ray contrast agent) and indocyanine green (ICG, NIR fluorescence dye), we optimize the hydrogel for prolonged localization at the injected site without losing the dual-imaging capability. We validate the effectiveness of the developed injectable dual-imaging platform by performing image-guided resection of pulmonary nodules on tumor-bearing rabbits, which are preoperatively localized with the hydrogel. The injectable dual-imaging marker, therefore, can emerge as a powerful tool for surgical guidance.

Received 8th January 2024,
Accepted 11th April 2024

DOI: 10.1039/d4bm00035h

rsc.li/biomaterials-science

Introduction

Computed tomography (CT)-guided preoperative localization and intraoperative identification of pulmonary nodules have garnered significant attention in regard to the widespread use of video-assisted thoracoscopic surgery (VATS).[1] VATS has become a standard method of minimally invasive procedures for the resection of pulmonary nodules when the percutaneous thoracic needle biopsy is impossible or resection of pulmonary nodules is required. Its wide application, however, is limited by the inability of clinicians to clearly distinguish lesions and the frequent requirement for intraoperative palpation due to lung collapsing.[2]

Several preoperative localization methods, such as hookwires, microcoils, radiotracers, radiocontrast agents, and dyes, have been developed to circumvent the shortfalls associated with VATS.[1,3–9] However, these methods suffer from drawbacks which include dislodgement (hookwires), radiation exposure to healthcare professionals (microcoils and radiocontrast agents), poor resolution (radiotracers), and rapid diffusion (dyes).

Indocyanine green (ICG) is one of the near-infrared (NIR) probes approved for determining cardiac output, hepatic function, and liver blood flow, and for use in ophthalmic angiography by the United States Food and Drug Administration (FDA). Therefore, it has been utilized in various clinical settings, for example, during lymphatic flow visualization, segmentectomy, or gastrointestinal conduit perfusion.[10,11] ICG has also been recently utilized for pulmonary nodule localization, as it can be clearly detected in the lung tissue even in the case of anthracosis while not hampering the surgeon's field of view.[1,12–17] However, the problem of rapid diffusion, being hydrophilic in nature, to surrounding tissues still remains as its unsolved limitation.[18] In addition, it suffers from a low tissue penetration depth of less than 1 cm, making the identification of deep-seated pulmonary nodules difficult.[19,20] Therefore, there is a necessity to develop an imaging contrast agent which can prevent dye leakage and allow the visualization of deep-seated pulmonary nodules. Recently, we intro-

[a]*Department of Bio and Brain Engineering and KAIST Institute for Health Science and Technology, Korea Advanced Institute of Science and Technology (KAIST), Daejeon, Republic of Korea. E-mail: jihopark@kaist.ac.kr*
[b]*Department of Thoracic and Cardiovascular Surgery, Korea University Guro Hospital, College of Medicine Korea University, Seoul, Republic of Korea. E-mail: kimhyunkoo@korea.ac.kr*
[c]*Department of Biomedical Sciences, College of Medicine Korea University, Seoul, Republic of Korea*
[d]*Department of Radiology, Korea University Guro Hospital, College of Medicine Korea University, Seoul, Republic of Korea*

†Electronic supplementary information (ESI) available. See DOI: https://doi.org/10.1039/d4bm00035h

‡These authors contributed equally to this work.

duced a fluorescent iodinated emulsion comprising a mixture of ICG solution and iodinated oil (Lipiodol®) for preoperative localization and intraoperative imaging in human subjects.[21] Although the emulsion had several advantages over other single-component dye localization materials in terms of dye leakage and penetration depth, inconsistent mixing caused by manual preparation methods and ICG leakage to surrounding normal tissues are drawbacks that still need to be overcome.[21]

Here, we report an injectable surfactant-free fluorescent and iodinated hydrogel for preoperative localization and dual image-guided surgery (Fig. 1). Hydrogel is a crosslinked polymer network comprising a large amount of water (typically 70–99%).[22] It has been leveraged in clinics as a drug delivery system due to its excellent biocompatibility and capability to encapsulate a variety of drugs.[22] Owing to their tunable physical and chemical characteristics such as gelation time and pore size, hydrogels can serve as a versatile platform for specific application-based requirements.[22,23] To this end, we synthesize a dextran-based injectable hydrogel, by utilizing the chemical principles of the thiol-Michael Addition Click reaction.[24,25] Dextran is a naturally occurring polysaccharide which has extensively been used in medicinal applications due to its biocompatibility.[26,27] The hydrogel containing both ICG and iodinated oil is optimized for visualization in the diseased tissue under both fluorescent and CT imaging. The effectiveness of the developed injectable hydrogel for use in preoperative localization and dual image-guided surgery is validated *in vivo*.

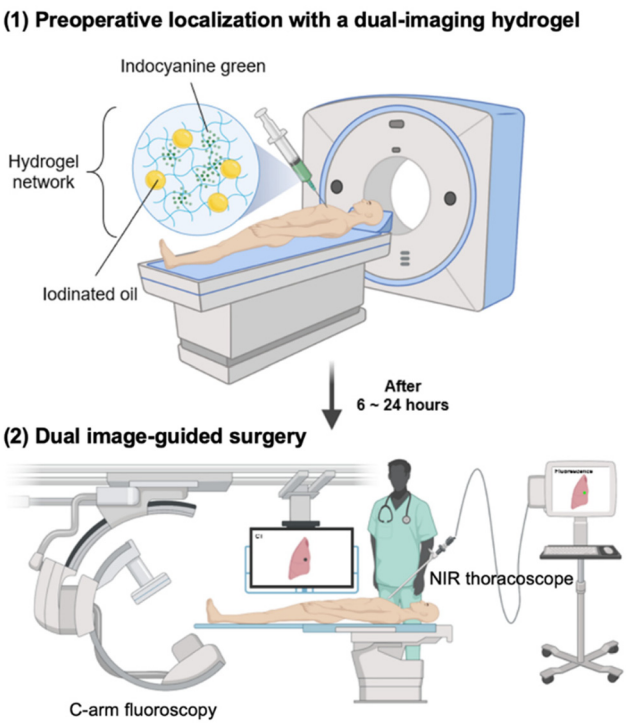

Fig. 1 Schematic illustration of preoperative localization and dual image-guided surgery of pulmonary nodules using an injectable fluorescent and iodinated hydrogel.

Materials and methods

Preparation of hydrogel precursors

Dextran-based injectable hydrogel precursors were synthesized according to previous literature.[25] Briefly, dextran was dissolved in 0.1 M NaOH at a concentration of 4% (w/v) and was reacted with 1.25× molar excess of divinyl sulfone under ambient temperature with continuous stirring. Different degrees of modification (DM) of dextran hydroxyl groups were achieved by controlling the reaction time. To stop the VS conjugation reaction, 6 M of HCl was added dropwise to the reaction mixture until pH became 4. The resulting solution was then dialyzed against deionized (DI) water for 3 days using Spectra/Por® dialysis membrane (MWCO: 3500 Da). Afterward, the solution was freeze-dried and subjected to ^{1}H Nuclear Magnetic Resonance (NMR) analysis by *Bruker Avance III™ HD 400 MHz NMR spectrometer*. The success of Dex-VS synthesis was confirmed by comparing the integral signals at $\delta = 6.9$ and $\delta = 2$.

Thiol-modified dextran (Dex-SH) was synthesized by first adding 1 M phosphate buffer to adjust the pH of the Dex-VS solution to 7.4. Then the solution was added with 5× molar excess of dithiothreitol (DTT) and reacted for 40 minutes under N_2 purging. The reaction was then stopped by lowering the pH of the reaction mixture to pH 4 by adding 1 M HCl. The resulting solution containing Dex-SH was dialyzed against an acidic medium (pH 4) using Spectra/Por® dialysis membrane (MWCO: 3500 Da) to remove residual DTT present in the mixture. After dialyzing for 3 days, the solution was freeze-dried for ^{1}H NMR analysis to check for the disappearance of VS signals. At the same time, the amount of chemically active thiol groups was quantified by Ellman's assay according to the manufacturer's protocol.

Formation of injectable fluorescent and iodinated hydrogels

Freeze-dried powders of Dex-VS and Dex-SH were respectively dissolved in phosphate-buffered saline (PBS) (pH 7.4) to the desired gelation concentrations. Indocyanine green (ICG, Daiichi-Sankyo Co., Tokyo, Japan) was added to each solution of Dex-VS and Dex-SH to the final concentration of 0.001% (w/v). Different volumes of iodinated oil (Lipiodol®) were also added to the respective solutions of hydrogel precursors. Afterward, each solution of Dex-SH and Dex-VS which contains the desired amounts of ICG and iodinated oil, were ultra-sonicated at 40 kHz for 10 minutes by using Branson 3510-DTH Ultrasonic Cleaner and were mixed to form a hydrogel. The gelation times of various hydrogels synthesized were determined by pipetting up and down method according to previous literature.[28] In brief, the time taken for the injectable hydrogel to clog the pipette tip was measured.

Physical characterization of hydrogels

The rheological properties of the hydrogels synthesized were measured with an Anton Paar rheometer. Parallel plates of 25 mm diameter were utilized in this study. To determine the storage (G') and loss (G'') moduli of hydrogels synthesized,

600 μl of hydrogel were gently placed in between the parallel plates with a gap height of 1 mm. Afterward, frequency sweep tests were performed in the frequency range spanning from 0.1 rad s^{-1} to 100 rad s^{-1} at 0.1% strain at 25 °C.

Emulsion stability index (ESI, %) measurements

The emulsion stability index (ESI, %) was calculated with slight modifications from the previous literature.[29] Upon gelation, the liquid volume of the emulsion was measured and the following equation was utilized to calculate ESI: ESI = $V_s/V_a \times 100\%$, where V_s is the volume of liquid emulsion and V_a is the total volume of the mixture before gelation.

Release profiles of ICG and iodinated oil

Pre-formed hydrogels containing ICG and iodinated oil were subjected to ICG fluorescence and CT signal measurements by IVIS Spectrum *In Vivo* Imaging System (PerkinElmer) and CT (Brilliance 64, Philips), respectively. Afterward, the hydrogels were incubated in a PBS reservoir for 24 hours at 37 °C, and any changes in fluorescent and CT signals were tracked and analyzed.

In vivo optimization of hydrogels in canine subjects

This animal experiment was approved and conducted in accordance with the guidelines provided by the Institutional Animal Care and Use Committee of Korea University College of Medicine (IACUC approval number: KOREA-2019-0175). Two male canines (Optipop; body weight, 30 kg) were used in the study. All canines were anesthetized by injecting 5 mg kg^{-1} of xylazine (Rompun™, Bayer Korea Inc Seoul) and zoletil (Zoletil™, Virbac) intramuscularly. To evaluate the degree of colocalizations, 0.2 ml of hydrogels containing different volume fractions of iodinated oil were injected into the pulmonary lobes of the canine using a 26-G needle under C-arm fluoroscopy (Koninklijke Philips). The C-arm and fluorescent images of lung surfaces were assessed using Pinpoint® thoracoscope (Novadaq Technologies Inc) and C-arm fluoroscopy (Koninklijke Philips). All lobes were then resected with an endostapler to take *ex vivo* images with Pinpoint and C-arm. Signals obtained from the region of interest were measured using Image J software (64-bit Java 1.8.0_172, National Institute of Health), and the signal of tumor-to-normal tissue ratio (TNR) was calculated.[30] The X-ray and fluorescent images of the same lobe were normalized against the image area to calculate the degree of colocalization.

In vivo imaging in rabbits

This animal experiment was approved and conducted in accordance with the guidelines provided by the Institutional Animal Care and Use Committee of Korea University College of Medicine (IACUC approval number: KOREA-2019-0175). A total of 2 female New Zealand White rabbits weighing between 2.5 kg and 3.0 kg were used in this study. The animals were purchased from Doo Yeol Biotech in South Korea and were housed in a metallic rabbit cage. Rabbits were maintained under controlled temperature, humidity, and illumination. Food and water were provided freely. Two rabbit lung tumor models were developed to confirm the effectiveness of the developed fluorescent and iodinated injectable hydrogel. Computed tomography (CT) guided injection of VX2 tumor tissues on a rabbit was performed to develop lung nodules as previously described.[31] During procedures, all animals were anesthetized by injecting 5 mg kg^{-1} of xylazine (Rompun™, Bayer Korea Inc Seoul) and zoletil (Zoletil™, Virbac) intramuscularly.

To check for the retentive tumor localization ability of the optimal hydrogel formulation comprising 20% (v/v) of iodinated oil, 0.2 ml of the hydrogel was injected at the periphery of a rabbit pulmonary nodule under fluoroscopic CT guidance. After 24 hours, a thoracotomy was performed. The X-ray and fluorescent imaging of lung surfaces was assessed using CT and our custom-manufactured intraoperative color and fluorescence-merged imaging system (ICFIS) as previously described.[19,20] *Ex vivo* images of the resected lobes were also imaged under CT and ICFIS.

Results

Preparation of an injectable fluorescent and iodinated hydrogel

The main objective of this study is to synthesize an injectable hydrogel that contains both ICG and iodinated oil for use in preoperative localization and image-guided surgery. As such, we synthesized vinyl sulfone- (Dex-VS) and thiol-modified dextran (Dex-SH) as hydrogel precursors, as gelation is triggered upon mixing these two precursors at physiological conditions due to the occurrence of the Michael addition reaction (Fig. 2A). Such hydrogels, however, are only applicable in clinical settings if the gelation time is fine-tuned to around 30 seconds, as hydrogels with faster or slower gelation times than 30 seconds would result in clogging of an injection needle or poor localization within the tissue, respectively (Fig. S1†). As such, we controlled two rate-determining parameters, specifically, degree of modification (DM) and gelation concentration (C_g), to screen for the optimal hydrogel formulation with the clinically relevant gelation time. In this regard, Dex-VSs with various DMs were synthesized by changing the reaction time while fixing the molar amount of divinyl sulfone and the pH. The DM by VS conjugation at different reaction times was calculated by analyzing ^{1}H NMR spectra by comparing the integral signals at δ = 6.9 and δ = 4.87–5.29 (Fig. S2†). We found an increase in the DM of Dex-VS with respect to the reaction time (Fig. 2B). In this manner, we synthesized three kinds of Dex-VS with different DMs (10%, 20%, and 30%), for further thiol conjugation and optimization. Dex-SH synthesis was performed by reacting Dex-VS with a 5× molar excess of thiol-containing dithiothreitol (DTT) to convert the entire VS moiety of Dex-VS to SH groups. The success of SH conjugation was confirmed by ^{1}H NMR and Ellman's assay (Fig. S3 and Table S1†). In addition to varying the DM, we controlled the polymer concentration which is another parameter that governs the gelation

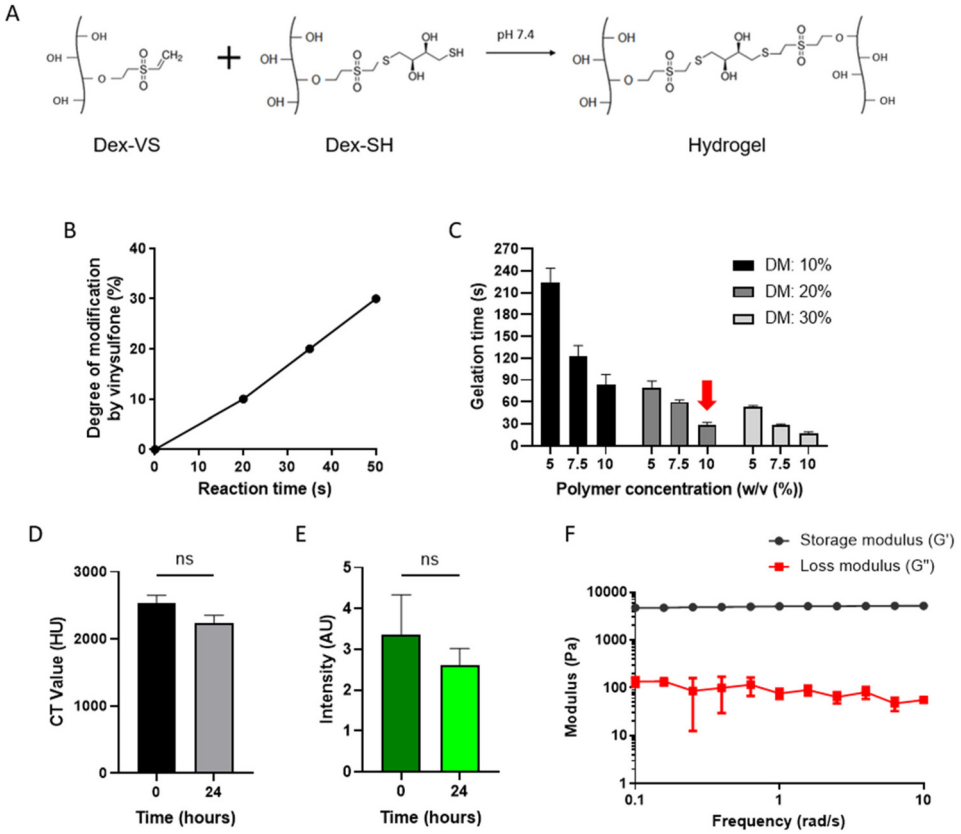

Fig. 2 Synthesis and characterization of an injectable fluorescent and iodinated hydrogel. (A) Chemical reaction scheme of the Michael Addition reaction occurring between vinyl sulfone (Dex-VS) and thiol-modified dextran (Dex-SH) forming an injectable hydrogel. (B) Synthesis of vinyl sulfone modified dextran precursors with different degrees of chemical modifications (%) by varying the reaction time. (C) Gelation times of hydrogels formed at various dextran precursor concentrations and DMs. The red arrow indicates the hydrogel formulation selected for preoperative localization (n = 6). (D) Comparison of CT signals before and after incubating a hydrogel (DM: 20%, concentration: 10% (w/v)) in PBS at 37 °C for 24 hours (n = 3). (E) Comparison of fluorescent signals before and after incubating a hydrogel (DM: 20%, concentration: 10% (w/v)) in PBS at 37 °C for 24 hours (n = 3). AU, arbitrary units. (F) Storage and loss modulus of the hydrogel (DM: 20%, concentration: 10% (w/v)) encapsulating 0.001% (w/v) ICG and 20% (v/v) iodinated oil (n = 3). The results were statistically analyzed by using an unpaired two-tailed Student's t-test. NS, not significant.

kinetics. We observed a decrease in the gelation time with respect to an increase in the DM and the gelation concentration (Fig. 2C). Two formulations, namely, a hydrogel with DM of 20% and C_g of 10% (w/v) and a hydrogel with DM of 30% and C_g of 7.5% (w/v), were found exhibiting the clinically desired gelation time of approximately 30 seconds (Fig. 2C, a red box). Among these two formulations, we selected the hydrogel with DM of 20% and C_g of 10% (w/v) as higher amounts of VS would decrease the solubility of Dex-VS while higher C_g would decrease the mesh size of the overall hydrogel network, which would eventually hinder the diffusion of an emulsion of iodinated oil and ICG solution.[25,32]

To formulate a hydrogel that can be utilized for preoperative CT and intraoperative dual imaging, we dissolved ICG in two aqueous solutions containing each hydrogel precursor. ICG concentration of 0.001% (w/v) was used in this study as the brightest fluorescence signal was visualized at this concentration according to previous literature.[33] On the other hand, we varied the volume fractions of iodinated oil in the precursor solution from 0% (v/v) to 30% (v/v) to determine the optimal amount of iodinated oil required for the gelation time and CT imaging. To check whether the incorporated iodinated oil would influence the gelation kinetics, different volume fractions of iodinated oil were mixed with the precursor solution containing the ICG, and ultrasonicated for 10 minutes prior to gelation. Afterward, gelation time was measured by mixing equal volumes of emulsified precursor solutions. Gelation time measurement by pipetting up and down method revealed that the incorporation of iodinated oil from 0 to 30% (v/v) had negligible effects on the gelation kinetics (Fig. S4†). At the same time, when the CT values of hydrogels containing different amounts of iodinated oil were measured, no enhancement in CT signals with respect to an increase in the volume fraction of iodinated oil was observed (Fig. S5†). Upon examining the structural integrity of the hydrogels, the formed hydrogel was physically separated from the oil phase when formulated with 30% (v/v) of iodinated oil (Fig. S6A and S6B†). To quantify such a phenomenon, we calculated an emulsion stability index (ESI, %) for the hydrogels. As expected, the hydrogel with 30% (v/v) of iodinated oil had an ESI of approxi-

mately 50% (unstable emulsion) while the hydrogels containing 10% (v/v) and 20% (v/v) of iodinated oil had an ESI of 100% (stable emulsion) (Fig. S6†).

As image-guided surgery is clinically performed after 6–24 hours of preoperative localization of pulmonary nodules, we examined whether the hydrogel can maintain CT and fluorescent signals *in vitro* during this period. The hydrogel containing 20% of iodinated oil was incubated in PBS at 37 °C for 24 hours and the CT value and the fluorescent intensity were measured before and after incubation. We observed no significant decrease in either CT value or fluorescent intensity after incubation (Fig. 2D and E). In addition, this hydrogel exhibited a higher storage modulus (G') of 5 kPa than a loss modulus (G'') of 100 Pa in all ranges of frequencies tested, indicating the successful formation of the elasticity-dominating hydrogel network (Fig. 2F). Based on these results, we proceeded to characterize the hydrogels containing 10% (v/v) and 20% (v/v) of iodinated oil in animal models.

In vivo optimization of injectable hydrogels in canine lungs

To characterize the dual-imaging property *in vivo*, each hydrogel containing ICG and 10% (v/v) or 20% (v/v) of iodinated oil was injected into the pulmonary lobes of canines under C-arm guidance (Fig. 3A). In both hydrogels, X-ray and fluorescent signals were detected under C-arm and Pinpoint while the control hydrogel without ICG and iodinated oil did not show any signals (Fig. 3B). The X-ray and fluorescent signals were also well detected on the resected lungs (Fig. 3C). Two hydrogels containing 10% (v/v) and 20% (v/v) of iodinated oil did not show significant difference in the fluorescent signals while the X-ray signal of the hydrogel with 20% (v/v) of iodinated oil was significantly higher than that of the hydrogel with 10%

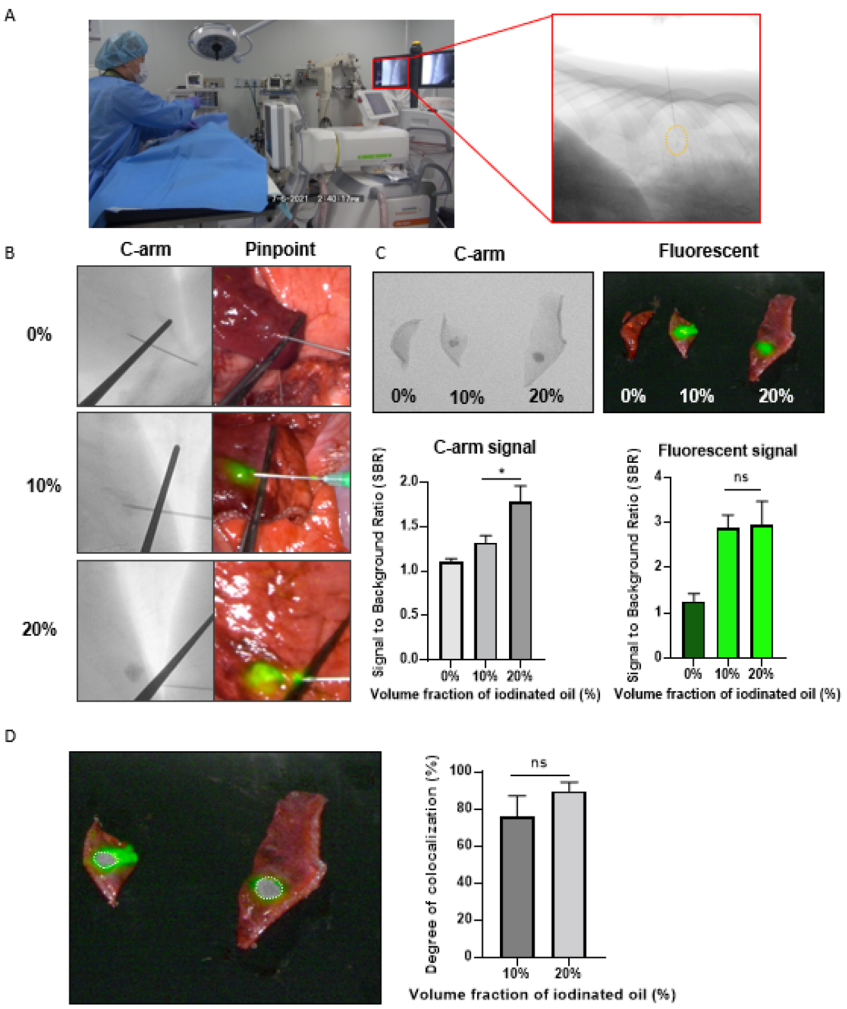

Fig. 3 *In vivo* optimization of injectable fluorescent and iodinated hydrogels in canine lungs. (A) C-arm guided hydrogel injection. (B) C-arm and fluorescent *in vivo* images right after injection of hydrogels which contain different volume fractions of iodinated oil (n = 3). (C) *Ex vivo* C-arm and fluorescent images after lung tissue resection with hydrogels with different concentrations of iodinated oil (n = 3). Signal to background ratios of the c-arm and fluorescent images. (D) Merged image of c-arm and fluorescent images, the green area indicates ICG, and the gray area with a white dotted line indicates iodinated oil. Degree of colocalizations between CT/X-ray and fluorescent signals were compared for two different hydrogels each containing 10% (v/v) or 20% (v/v) of iodinated oil, respectively. The results were statistically analyzed by using an unpaired two-tailed t-test. NS, not significant.

(v/v) of iodinated oil. No statistically significant difference was noted upon examining the degree of colocalizations between CT/X-ray and fluorescent signals on the resected lungs injected with the two hydrogels (Fig. 3D). This result indicates that hydrogels were well-formed regardless of the volume fractions of iodinated oil. However, the hydrogel with 20% (v/v) of iodinated oil was chosen as an optimized formulation owing to its stronger X-ray signal (see Movie S1†).

Preoperative localization and dual image-guided surgery of pulmonary nodules using an injectable hydrogel

To perform the preoperative localization and dual image-guided surgery of pulmonary nodules, a VX2 tumor with globular structures was first developed in the rabbit lung (Fig. 4A). After that, the hydrogel containing ICG and iodinated oil was injected around the pulmonary nodule under C-arm guidance (Fig. 4B). CT images demonstrated that the hydrogel was well localized at the periphery of the tumor immediately after injection and retained its signal intensity for 24 hours upon CT-guided preoperative localization (Fig. 4C). Intraoperative fluorescence imaging at 24-hour post-localization revealed that the fluorescence signal of the hydrogel was also clearly detected in the nodule region. The CT and fluorescence signals were also sufficiently bright for tumor localization. *Ex vivo* dual imaging of the resected lung tissue also confirmed that the X-ray and fluorescence signals of the hydrogel were co-localized in the nodule without significant separation (Fig. 4D). These results demonstrated the localization ability of the optimized hydrogel-based dual imaging platform in the pulmonary nodule and for use in image-guided surgery.

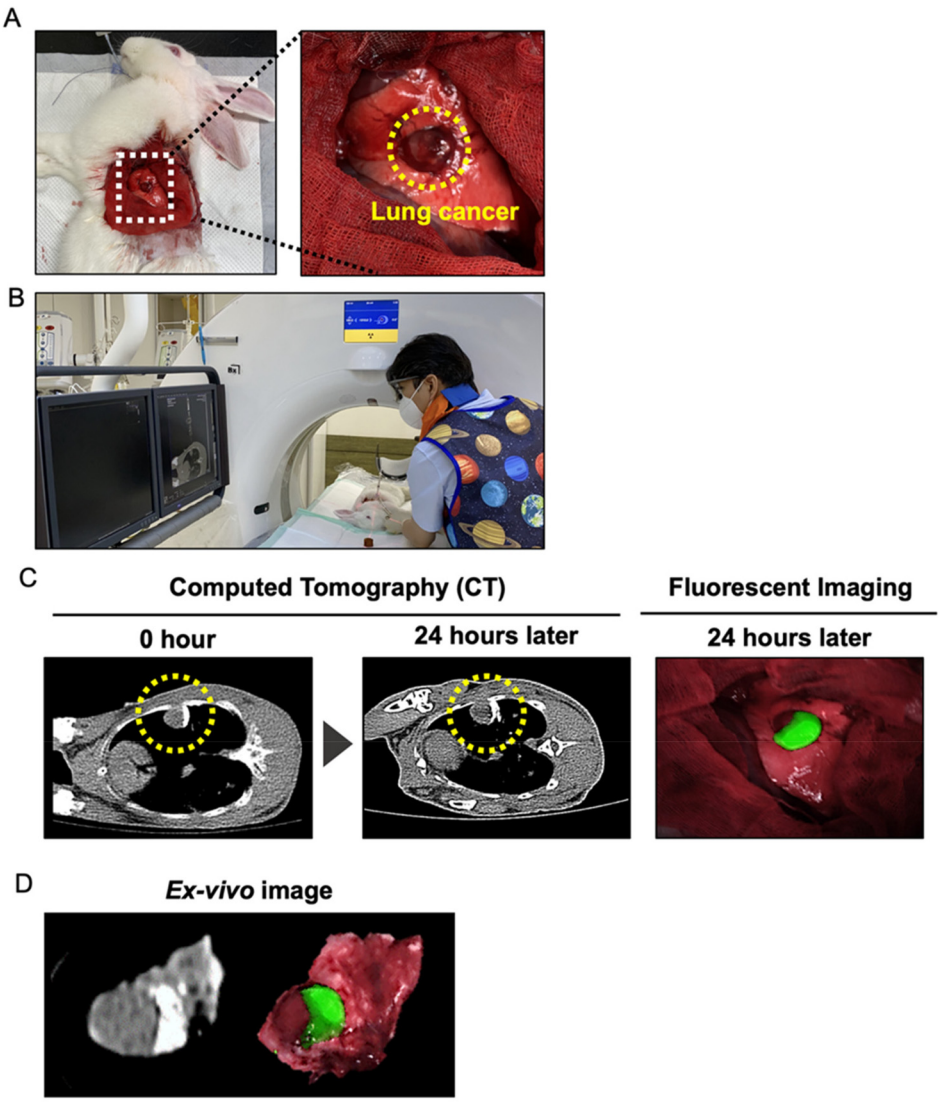

Fig. 4 Pulmonary nodule localization by the optimized hydrogel *in vivo* and dual image-guided surgery. (A) Rabbit lung cancer model. (B) CT-guided injection of the optimized hydrogel. (C) CT and fluorescent images after 24 hours of CT-guided injection of the optimized hydrogel. (C) CT and fluorescent images after 24 hours of CT-guided injection of the optimized hydrogel. (D) C-arm and fluorescent *ex vivo* images of resected lung cancer identified by the optimized hydrogel.

Discussion

In this study, we developed an injectable fluorescent and iodinated hydrogel for use in preoperative pulmonary localization and intraoperative dual-imaging of deep-seated nodules which can overcome the disadvantages of conventional localization techniques, such as dye leakage to normal tissues and poor penetration depth (Fig. 1).[18–20] Dextran was utilized to synthesize the hydrogel network for its well-known biocompatibility. For hydrogel synthesis, we exploited the Michael addition Click chemistry specifically by substituting the hydroxyl groups of dextran with vinyl sulfone and thiol groups, respectively.[25,34] The simple click method enables the polymers to become clickable under physiological conditions thereby making it suitable for a wide range of biomedical applications (Fig. 2A). Further, to clinically apply the hydrogel, we carefully engineered the gelation time of the hydrogel to 30 seconds, as hydrogels with faster or slower gelation times than 30 seconds would result in clogging of an injection needle or poor localization within the tissue. As such, we controlled two rate-determining parameters, specifically, degree of modification (DM) and gelation concentration (C_g), to screen for the optimal hydrogel formulation with the clinically relevant gelation time. Consistent with previous literature, the gelation kinetics exhibited a positive correlation with both parameters. Two hydrogel formulations exhibited a gelation time of approximately 30 seconds (Fig. 2C). Among them, we selected the hydrogel with DM of 20% and C_g of 10% (w/v) for further optimizations as higher amounts of VS would decrease the solubility of Dex-VS while higher C_g would decrease the mesh size (ξ_m) of the overall hydrogel network.[25,32] Consequently, these hydrogel properties were expected to hinder the aggregation and diffusion of emulsions.

FDA-approved imaging agents, ICG, and iodinated oil were chosen to prepare the injectable dual-imaging hydrogel. ICG was incorporated in the hydrogel at the concentration which has been demonstrated to exhibit the brightest fluorescent signal.[33] Iodinated oil was emulsified with the ICG-incorporated hydrogel precursors to form a hydrogel with 20% (v/v) of iodinated oil. Higher oil content, for example, at 30% (v/v), resulted in the reduction of the emulsion stability index as indicated by the phase separation between the solid hydrogel and the oil (Fig. S6†). On the other hand, the hydrogel containing the iodinated oil with a volume fraction lower than 20% (v/v) was not considered for further investigation due to low CT signal *in vivo* (Fig. 3B). These results indicate that the volume fraction of iodinated oil should be 20% (v/v) for preparing a highly stable emulsion-filled hydrogel with strong dual imaging signals.

Hydrogels are known to prevent flocculation and coalescence of emulsion droplets by immobilizing the droplets within the gel structure.[35] In line with this, the dual-imaging ability and localization stability of the hydrogel containing an emulsion of ICG and iodinated oil were tested both *in vitro* and *in vivo*. Upon incubation in PBS at 37 °C for 24 hours, the hydrogel showed no significant reductions in both CT value and fluorescent intensity (Fig. 2D and E), and no physical change such as phase separation phenomenon (Fig. S6†) occurred as indicated by no ICG and iodinated oil leakage from the hydrogel.

In addition, the optimized fluorescent and iodinated hydrogel had a storage modulus of approximately 5 kPa which is comparable to the stiffness of various tissues in the body (Fig. 2F).[36] When injected in the lung tissues under CT guidance, both fluorescence and X-ray/CT signals were clearly detected from the injected site 24 hours post-injection (Fig. 3B, 4A and C), indicating that the hydrogel was immediately formed and localized in the tissue without physical separation. Further, when the *ex vivo* images of the resected lung nodule were analyzed, colocalization of both fluorescent and CT signals was observed (see Movie S1† and Fig. 3D and 4D), thus reflecting the ability of the developed hydrogel for use in pulmonary nodule identification with dual imaging and image-guided surgery.

Conclusions

We developed a versatile hydrogel-based platform capable of preoperative localization and intraoperative dual imaging of pulmonary nodules. The injectable hydrogel with CT/X-ray and fluorescence dual imaging capability was optimized for deep pulmonary nodule identification by carefully controlling the gelation time and the volume fraction of iodinated oil in the hydrogel. The results obtained in this study warrant further clinical trials on human subjects to validate the effectiveness of the developed injectable fluorescent and iodinated injectable hydrogel.

Author contributions

Woojin Back: Conceptualization, methodology, validation, formal analysis, investigation, data curation, writing – original draft. Jiyun Rho: Conceptualization, methodology, validation, formal analysis, investigation, data curation, writing – original draft. Kyoung Su Kim: Methodology. Hwan Seok Yong: Methodology. Ok Hwa Jeon: Methodology. Byeong Hyeon Choi: Methodology. Hyun Koo Kim: Conceptualization, Methodology, writing – original draft, supervision, funding acquisition. Ji-Ho Park: Conceptualization, methodology, writing – original draft, supervision, funding acquisition.

Conflicts of interest

There are no conflicts to declare.

Acknowledgements

This study was supported by the Korean Association for Lung Cancer Research Grant 2019, and supported by a grant of the

Korea Health Technology R&D Project through the Korea Health Industry Development Institute (KHIDI), funded by the Ministry of Health & Welfare, Republic of Korea (grant number: HI20C0835). This work was also partially supported by ETRI (Electronics and Telecommunications Research Institute)'s internal funds [22YR1900, Development of Digital Biopsy Core Technology for high-precision Diagnosis of Senile Disease].

References

1 J. Rho, J. W. Lee, Y. H. Quan, B. H. Choi, B. K. Shin, K. N. Han, B. M. Kim, Y. H. Choi, H. S. Yong and H. K. Kim, *Ann. Surg.*, 2021, **273**, 989–996.
2 B. A. Whitson, S. S. Groth, S. J. Duval, S. J. Swanson and M. A. Maddaus, *Ann. Thorac. Surg.*, 2008, **86**, 2008–2018.
3 B. Kidane and K. Yasufuku, *Thorac. Surg. Clin.*, 2016, **26**, 129–138.
4 C. H. Park, K. Han, J. Hur, S. M. Lee, J. W. Lee, S. H. Hwang, J. S. Seo, K. H. Lee, W. Kwon, T. H. Kim and B. W. Choi, *Chest*, 2017, **151**, 316–328.
5 M. W. Lin and J. S. Chen, *J. Thorac. Dis.*, 2016, **8**, S749–S755.
6 J. Keating and S. Singhal, *Semin. Thorac. Cardiovasc. Surg.*, 2016, **28**, 127–136.
7 H. K. Kim, W. M. Jo, J. H. Jung, W. J. Chung, J. H. Shim, Y. H. Choi and I. S. Lee, *Ann. Thorac. Surg.*, 2008, **86**, 1098–1103.
8 K. W. Doo, H. S. Yong, H. K. Kim, S. Kim, E. Y. Kang and Y. H. Choi, *Ann. Surg. Oncol.*, 2015, **22**, 331–337.
9 D. Y. Kang, H. K. Kim, Y. K. Kim, H. S. Yong, E. Y. Kang and Y. H. Choi, *Eur. Respir. J.*, 2011, **37**, 13–17.
10 J. Zhou, F. Yang, G. Jiang and J. Wang, *J. Thorac. Dis.*, 2016, **8**, S738–S743.
11 A. L. Vahrmeijer, M. Hutteman, J. R. Van Der Vorst, C. J. H. Van De Velde and J. V. Frangioni, *Nat. Rev. Clin Oncol.*, 2013, **10**, 507–518.
12 C. T. Wen, Y. Y. Liu, H. Y. Fang, M. J. Hsieh and Y. K. Chao, *Surg. Endosc.*, 2018, **32**, 4673–4680.
13 A. Abbas, S. Kadakia, V. Ambur, K. Muro and L. Kaiser, *J. Thorac. Cardiovasc. Surg.*, 2017, **153**, 1581–1590.
14 T. Anayama, K. Hirohashi, R. Miyazaki, H. Okada, N. Kawamoto, M. Yamamoto, T. Sato and K. Orihashi, *J. Cardiothorac. Surg.*, 2018, **13**, 1–8.
15 H. Ujiie, T. Kato, H. pei Hu, P. Patel, H. Wada, K. Fujino, R. Weersink, E. Nguyen, M. Cypel, A. Pierre, M. de Perrot, G. Darling, T. K. Waddell, S. Keshavjee and K. Yasufuku, *J. Thorac. Cardiovasc. Surg.*, 2017, **154**, 702–711.
16 K. J. Hachey, C. S. Digesu, K. W. Armstrong, D. M. Gilmore, O. V. Khullar, B. Whang, H. Tsukada and Y. L. Colson, *J. Thorac. Cardiovasc. Surg.*, 2017, **154**, 1110–1118.
17 S. L. Hillary, S. Guillermet, N. J. Brown and S. P. Balasubramanian, *Langenbecks Arch. Surg.*, 2018, **403**, 111–118.
18 A. Trakarnsanga, *World J. Gastrointest. Endosc.*, 2011, **3**, 256.
19 B. Partik, A. N. Leung, M. Müller, M. Breitenseher, F. Eckersberger, G. Dekan, T. H. Helbich and V. Metz, *Am. J. Roentgenol.*, 2003, **180**, 805–809.
20 K. Suzuki, K. Nagai, J. Yoshida, H. Ohmatsu, K. Takahashi, M. Nishimura and Y. Nishiwaki, *Chest*, 1999, **115**, 563–568.
21 J. Rho, J. W. Lee, Y. H. Quan, B. H. Choi, B. K. Shin, K. N. Han, B. M. Kim, Y. H. Choi, H. S. Yong and H. K. Kim, *Ann. Surg.*, 2021, **273**, 989–996.
22 J. Li and D. J. Mooney, *Nat. Rev. Mater.*, 2016, **1**, 1–17.
23 P. Calvert, *Adv. Mater.*, 2009, **21**, 743–756.
24 C. E. Hoyle and C. N. Bowman, *Angew. Chem., Int. Ed.*, 2010, **49**, 1540–1573.
25 Y. Yu and Y. Chau, *Biomacromolecules*, 2012, **13**, 937–942.
26 Q. Zhu, B. Bao, Q. Zhang, J. Yu and W. Lu, *RSC Adv.*, 2018, **8**, 2818–2823.
27 R. D. Hamstra, M. H. Block and A. L. Schocket, *JAMA*, 1980, **243**, 1726–1731.
28 C. K. Chung, M. F. Fransen, K. van der Maaden, Y. Campos, J. García-Couce, D. Kralisch, A. Chan, F. Ossendorp and L. J. Cruz, *J. Controlled Release*, 2020, **323**, 1–11.
29 W. S. Annan, M. Fairhead, P. Pereira and C. F. V. Der Walle, *Protein Eng., Des. Sel.*, 2006, **19**, 537–545.
30 H. K. Kim, Y. H. Quan, C. H. Oh, D. Jung, J. Y. Lim, B. H. Choi, J. Rho, Y. Choi, K. N. Han, B. M. Kim, C. Kim and J. H. Park, *JAMA Surg.*, 2020, **155**, 732–740.
31 B. H. Choi, H. S. Young, Y. H. Quan, J. Rho, J. S. Eo, K. N. Han, Y. H. Choi and K. H. Koo, *PLoS One*, 2017, **13**, e0192527.
32 Y. Yu and Y. Chau, Biomacromolecules, 2015, **16**, 56–65.
33 H. Wada, K. Hirohashi, T. Anayama, T. Nakajima, T. Kato, H. H. L. Chan, J. Qiu, M. Daly, R. Weersink, D. A. Jaffray, J. C. Irish, T. K. Waddell, S. Keshavjee, I. Yoshino and K. Yasufuku, *PLoS One*, 2015, **10**, e0126945.
34 C. E. Hoyle and C. N. Bowman, *Angew. Chem., Int. Ed.*, 2010, **49**, 1540–1573.
35 T. Farjami and A. Madadlou, *Trends Food Sci. Technol.*, 2019, **86**, 85–94.
36 C. F. Guimarães, L. Gasperini, A. P. Marques and R. L. Reis, *Nat. Rev. Mater.*, 2020, **5**, 351–370.

